Laser Surface Texturing to Improve EB-PVD Thermal Barrier Coating Adhesion

Lucille Després[1,2], Sophie Costil[1], Florent Mauget[3], Romain Cariou[2], Aurélien Joulia[2], Amar Saboundji[2], Lorena Mataveli Suave[2] and Jonathan Cormier[3]

[1] Université de Bourgogne Franche-Comté - UTBM, Laboratoire Interdisciplinaire Carnot de Bourgogne, UMR 6303 CNRS, 90100 Belfort

[2] Safran Tech, Plateforme Aubes de Turbine avancées, 171 boulevard de Valmy, 92700 Colombes

[3] Institut Pprime, UPR CNRS 3346, Département de Physique et Mécanique des Matériaux, ISAE-ENSMA, 1 avenue Clément Ader, BP 40109, 86961 Futuroscope-Chasseneuil

FRANCE

jonathan.cormier@ensma.fr

Keywords: Thermo-Mechanical Fatigue Durability, Interfacial Cracking, Laser Texturing, Burner Rig Testing.

ABSTRACT

The development of internal cooling networks in HP (high pressure) blades coupled with the use of thermal barrier coating allows increasing the turbine entry temperature of aero-engines in order to improve their efficiency. A thermal barrier system, which is composed of three different layers deposited on a nickel-based superalloy substrate, is subjected during service to complex thermo-mechanical loading paths. The resulting damage mechanisms may lead to a premature spallation of the topcoat and a substantial deterioration the overall durability of the system. To ensure a mechanical anchoring between layers leading to increased time to spallation of the topcoat, different patterns have been developed on the bond coat by laser texturing. After surface morphology optimization, damage mechanisms of the textured thermal barrier coating systems are presented.

1.0 INTRODUCTION

Original engine makers have to design even more efficient aero-engines, with a reduced environmental impact in terms of NOx and CO/CO_2 emissions, while lowering production costs [1]. To meet such environmental requirements, in addition to a decrease in the specific fuel consumption, the temperature at the entry of the turbine has to be increased. The optimized aero-engines thermodynamic efficiency to meet such requirements hence results in more and more demanding operating conditions in terms of mechanical (creep, fatigue) and environmental (oxidation, corrosion) damages of high-pressure (HP) turbine blades and vanes. To achieve such improvements, the chemical composition of nickel-based superalloys is constantly being optimized to improve their resistance to oxidation and to improve their mechanical strength at high temperatures [2-5]. The processes used to obtain these castings have greatly evolved, allowing them to move from polycrystalline structures to columnar and then single-crystalline (SX) structures, thus improving their resistance to creep at high temperatures, in addition to improved investment casting techniques leading to the possibility of introducing intricate internal cooling channels of HP turbine blades [6, 7].
Turbine blades of the most advanced aero-engines are usually coated with a thermal barrier coating (TBC) system allowing the temperature felt by the metallic substrate to be lowered by typically 50 to 150 °C, depending on the ceramic top-coat thickness. This system is generally composed of three distinct layers namely a bond coat ensuring the bond between the metallic substrate and the ceramic layer, a natural oxide layer called TGO (thermally grown oxide), and a ceramic layer providing thermal insulation. A lot of work

on the design of thermal barrier systems is of course always carried out to improve their intrinsic properties but also to improve their service life. Indeed, thermal barrier systems are continuously subjected to high thermal and mechanical stresses. Among the several damage mechanisms, ceramic coating spallation can be catastrophic for the service life of turbine blades [8, 9, 10]. Indeed, the superalloy would then subject to temperatures close to its melting point. Likewise, as soon as the oxide layer delaminates, the phenomenon of interdiffusion of the elements between the layers of the system accelerates, causing the protective oxide layer to grow, depleting the superalloy of the γ'-generating elements and thus affecting the stability of the superalloy at high temperatures. Within this context, improving the in-service performances of thermal barrier systems and slowing down the kinetics spallation of the ceramic layer is one of the targets to be reached. In the present work, it was chosen to strengthen the mechanical anchoring between the layers of the thermal barrier system. This anchoring is often favored by high roughness at the interface between the ceramic layer and its substrate, which in the field of TBCs is often provided by sandblasting. However, apart from the problems of surface contamination, such a process does not allow fine control of the surface geometry. This is precisely why a laser texturing process has been tested in order to check whether it would be possible to strengthen the mechanical adhesion and to avoid premature spallation of the ceramic layer in service. Such a laser patterning of the surface has already been shown by Smialek et al. to be efficient for the improvement of the thermal cycling life of a thermally sprayed topcoat (TC) over a standard bond coat/superalloy substrate [11].

While such effects were already promising in the case of plasma sprayed YSZ layers on a 1st generation single crystal AM1 superalloy without any bond coat [11], it is no longer possible to determine whether such treatments could be as favorable in the case of a complete system with a bond coat and a TC deposited by electron-beam phase vapor deposition (EB-PVD) process. To answer this question, it is then necessary to study the growth of yttria partially stabilized zirconia (YSZ) columns on various surface morphologies in order to control the microstructure of this protective layer. Finally, thermal cycling tests were carried out to discriminate the generated surface morphologies. In addition, since HP turbine blades are subjected in service to complex thermal and mechanical stresses including, for example, creep, oxidation and thermomechanical fatigue at high temperatures the performances of a textured TBC system compared to the non-textured one have been tested in out-of-phase (OP) thermo-mechanical fatigue tests in simulated engine environment using the MAATRE burner rig [12-15]. The overall goal of this study is to try to develop a full TBC system with improved durability at very high temperature, by improving the time to top-coat spallation.

2.0 MATERIALS AND METHODS

2.1 Materials and Treatments

This study was carried out using the recently developed CMSX4 Plus superalloy (3rd generation Ni-based single crystal superalloy) [16]. The composition of this Ni-base single crystal superalloy casted into rods using a standard Bridgman process, is given in Table 1. Standard solution heat treatments were then supplied to reach aged materials [16]. These standard heat treatment sequences allowed to obtain a classical cuboidal γ/γ' morphology with γ' precipitates having an average 0.4-0.5 µm edge length (Fig. 1-a). Tubular specimens having geometries similar to the ones previously used by Mauget et al. were used in the present study [13,14]. These specimens were machined out from these rods close to a <001> crystallographic orientation (primary misorientation less than 8 degrees).

The γ/γ' bond coat has a thickness of about twenty micrometers (Fig. 1-b) [25]. It was deposited on the substrate by a process of physical vapor deposition (PVD) by co-evaporation. After deposition of the bond coat, a heat treatment of 4 hours at 1100°C is carried out in order to allow the interdiffusion of the elements between this bond coat and the substrate.
The natural oxide layer called TGO is formed in a preheating lock of the EB-PVD chamber. This oxidation

treatment, which lasted about 20 min, formed a layer of α-phase alumina between 400 and 600 nm thick. The thermal barrier coating used in this work was yttria (8% by mass) partially stabilized zirconia. It had a thickness of about 150 µm and a columnar structure. The deposition of the thermal barrier coatings on different samples was carried out by the EB-PVD process according to the industrial process of the Ceramic Coating Center in Châtellerault, France. Figure 2 shows the thermal barrier coating deposited on the γ/γ' bond coat.

Table 1. Chemical composition of CMSX4 Plus single crystal superalloy.

Solvus	Density (g/cm^3)	Composition (wt. %)								
		Ni	Co	Cr	Mo	W	Ta	Al	Ti	Re
1334+/-5	8.93	Bal.	10	3.5	0.6	6.0	8.0	5.7	0.9	4.8

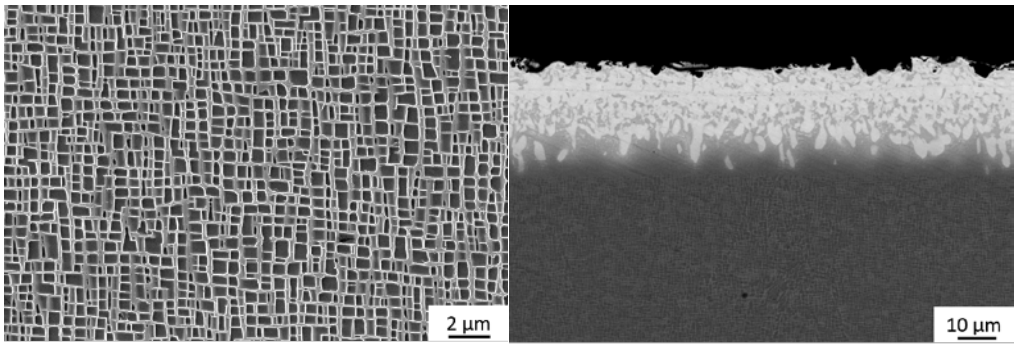

Figure 1: Standard microstructure of a) CMSX4 Plus; b) γ/γ' bond coat.

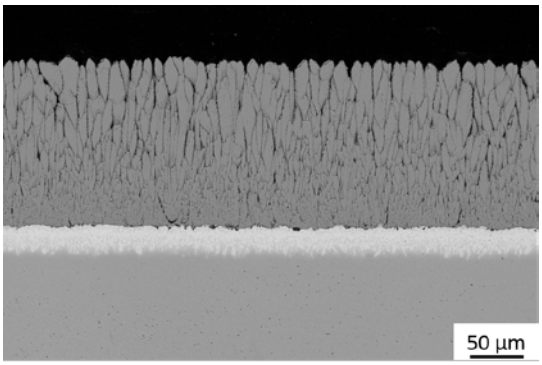

Figure 2: EB-PVD columns developed on the bond coat.

Regarding surface preparation, specimens were laser textured with a pulsed fiber laser (Laseo, Ylia M20, Quantel France) to structure the surface [15]. The laser operated at a nominal wavelength of 1.06 µm with a pulse duration of 100 ns, a maximum power of 20W and variable frequency varying between 10 and 100 kHz. The laser beam used for this study was circular with a diameter of 60 µm at the focal point and a gaussian energy distribution. Using this process, it is possible to generate different patterns composed of

holes or grids on substrate surfaces. Various variants from the point of view of shapes, depths, diameters, beads of material or even spacing between patterns have therefore been obtained (Table 2).

2.2 Characterizations Methods

After optimization of the surface morphologies, it was therefore fundamental to verify if the generated morphologies had an influence on the adhesion mechanisms and consequently on the spallation resistance of the thermal barrier systems. Thermal cycling tests were therefore carried out on the thermal barrier systems considered for this study in order to evaluate their spallation lifetime. The thermal cycle applied on coated samples was: 1. temperature rise (up to 1150°C) for 15 minutes; 2. holding temperature (1150°C) for 60 minutes; 3. air quench plus holding the sample at room temperature for 15 min. The test was stopped when about 20% (by surface area) of the topcoat was spalled. Three coated samples were tested for each condition to assess a mean value. By comparing the lifetimes, it becomes possible to check whether the optimized interface morphologies reinforce the adhesion of the ceramic layer on the γ/γ' bond coat.

Table 2: Morphologies of texturing conditions tested.

Conditions	1	2	3	4	7	Hole pattern
Depth [µm]	54	20	20	12	30	
Internal Diameter [µm]	53	70	40	40	23	
Conditions	5	6				Grids
Range [µm]	10	6				
Regularity [µm]	60	40				

In order to study the oxidation kinetics as a function of the surface treatment applied to the sample, isothermal oxidation tests of 100 h at 1150°C were then carried out by a modular thermogravimetric analyzer (ATG SETARAM SETSYS). The measurement of mass change was done with an accuracy of 1 µg. For this purpose, 1-mm-thick, 13-mm-diameter pins with 1-mm chamfers on both ends were machined. After texturing or sandblasting treatment, both ends of the pins were thus coated via a specific tooling.

Finally, out-of-phase thermomechanical fatigue tests on cooled tubular specimens were carried out on the MAATRE bench (Pprime Institute, Poitiers France) with the aim of evaluating the resistance of thermal barrier systems under complex stresses close to those encountered in service [14, 15]. This is a very unique burner rig whose aim is to reproduce the conditions encountered by components such as blades, vanes, shrouds in the hottest sections of aero-engines [12-15, 20]. The internal cooling of the specimens thus generates multi-axial thermal gradients within the specimen which can have a major impact on the performance of the specimens during such test as well as on the mechanism of the test associated damage. The term "leading edge" is used to refer to the portion of the specimen that is facing the flame during testing while the opposite face of the tubular specimen will be called “trailing edge” (Fig. 3). As such, our tubular specimens are able to represent during one single test the mechanical behavior of both the pressure and suction sides of a blade, as well as the mechanical stress state across the thickness of components.

The loading conditions applied to the tubular specimens during these tests were: 1. temperature rise: 60s/20°C.s^{-1}; 2. hot bearing: 1h/-100 MPa/Tmax= 1150°C at the leading edge; 3. descent in temperature: 60s/20°C.s^{-1}; 4. cold bearing: 30s/+700 MPa/500°C. An internal cooling was applied to the system to achieve a through-thickness representative thermal gradient [20]. These conditions were chosen to represent the mechanical behavior of "hot spots" of airfoils, during a critical regime of a flight.

In order to analyze the different samples after testing, it was necessary to carry out a series of steps to prepare them and thus facilitate observations. Morphologies and microstructures were evaluated with a scanning electron microscope (SEM) (JEOL 6400, 7000F, 7800F) on the surface or from etched (10 seconds with aqua regia (1/3 HNO_3 + 2/3 HCl by volume)) cross-sectional sample. In order to measure the geometries, at least six SEM images of each textured pattern, at x1000 magnification, were processed by the ImageJ software.

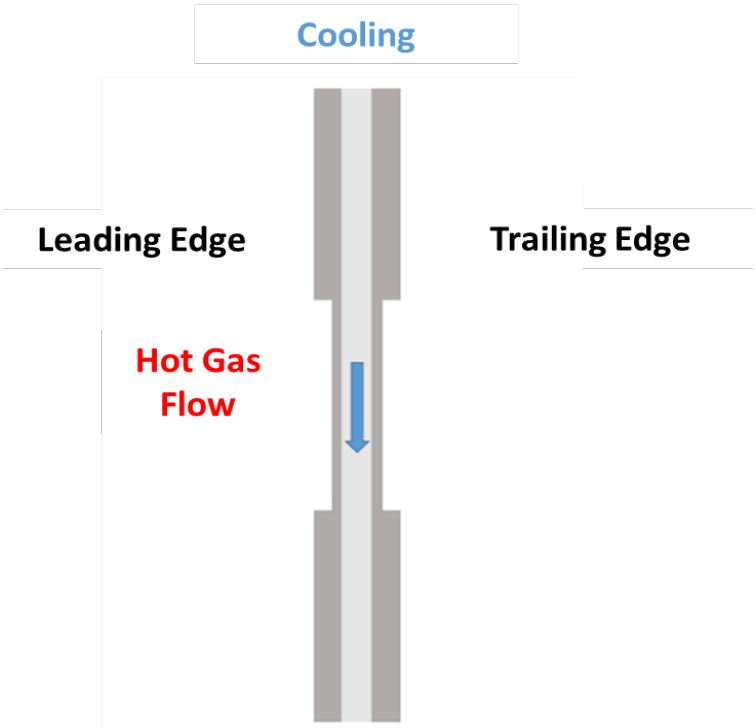

Figure 3: Edges denominations during specimen testing.

3.0 RESULTS AND DISCUSSION

Varying laser parameters, several surface morphologies were designed on the γ/γ' bond-coat as hole patterns or grids with different characteristics (see Fig. 4). Because PVD coatings strongly follow the surface variations, specific surface morphologies were then selected to focus the standard PVD coating as a reference. In order to avoid shadowing phenomena, different criteria were therefore verified in terms of depth/opening of cavities, surface irregularities, spatial distribution of irregularities. To illustrate the tested surfaces, Fig. 4 exhibits the textured samples on both the (a) surface and (b) cross-section as well as (c) after the coating buildup in the cross-section.

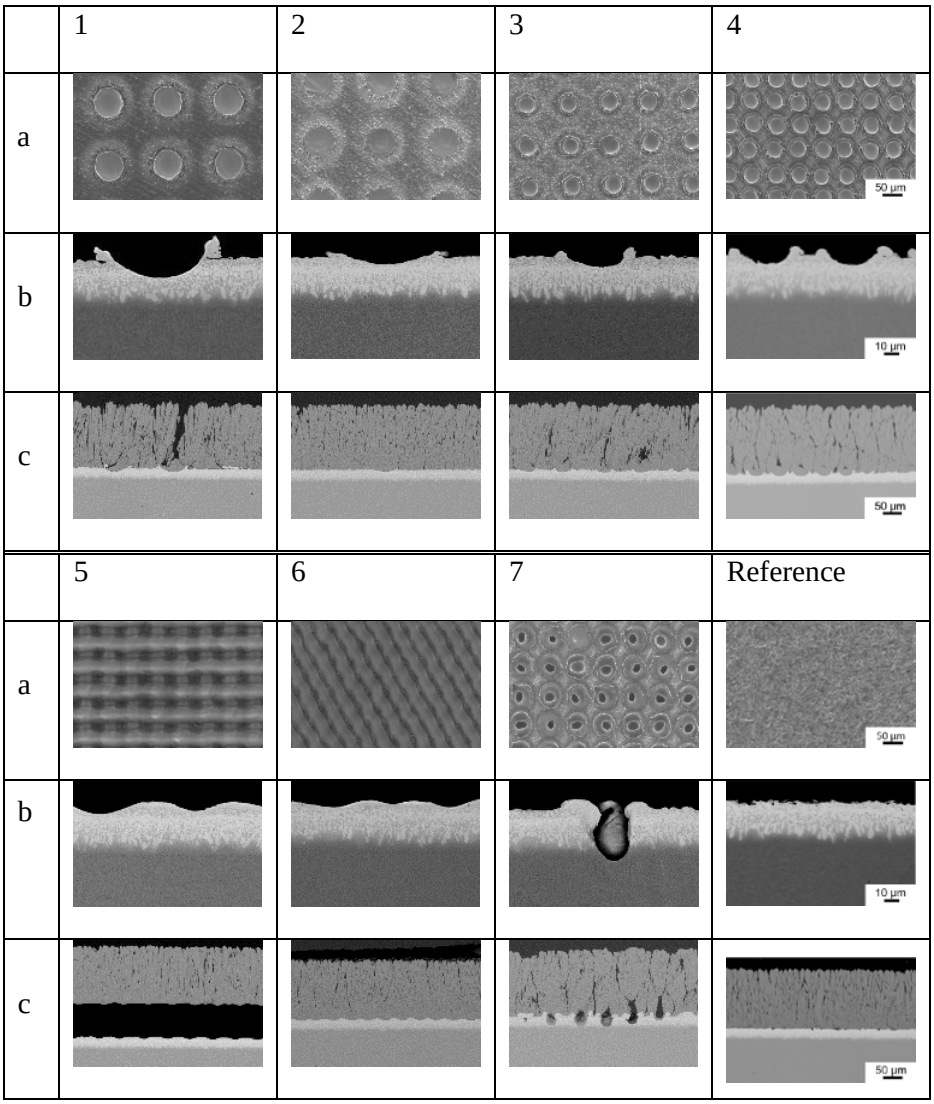

Figure 4: SEM observations of textured materials – a) on the surface; b) on the cross-section and (c) after coating buildup in the cross-section.

Different morphologies have been developed presenting various irregularities on the surface. Considering the γ/γ' layer, most of the treatments were limited in the thickness excepted for condition 7 which went through the bond-coat. Nevertheless, whatever the surface morphologies, deposited topcoat structures relatively close to the reference condition have been observed. The coating density of the deposits is quite similar (98.6 +/- 0.2%) for all conditions. Regarding the intercolumn void fraction, except for condition 1 which presents a high level of ~25%, surface morphologies seem favorable to maintain the percentage to 10%. It is now becoming essential to verify the extent to which these morphologies have an impact on the spallation resistance of thermal barrier systems during thermal and thermomechanical cycling.

Using thermal cycling tests, the behavior of EB-PVD coatings on surfaces with specific morphologies were therefore carried out. Table 3 shows the lifetimes achieved by the different configurations when about 20% of the topcoat is spalled. Such a criteria has been used as further spallation of the top coat is extremely fast. Except for the textured thermal barrier coating (TBC) system N°7, all textured TB systems have caused premature spallation with respect to the reference (non-textured, i.e., sandblasted) that has reached lifetimes close to 900 cycles. The lifetimes of the textured system N°7 in these thermal cycling tests appear to be equivalent or even superior to those of the sandblasted reference system. The influence of the surface

morphology thus seems to deeply control the thermal cycling behavior of such systems. It is therefore quite relevant to look at the damage mechanisms that may have led to the spallation of the coating. According to the literature about cyclic thermal loading, spallation of the ceramic TC is closely related to the coupled deformations of the oxide layer and the bond-coat [17, 18, 19, 22]. As illustrated in Fig. 5, there are different mechanisms of oxide growth involved. Indeed, some surface morphologies seem to favor the growth of a single oxide layer while others favor different types of oxides. Phase contrasts, underlined by gray gradients at the TGO level, reveal several oxides.

Table 3. Cyclic oxidation results at 1150°C. Standard deviations are extracted from the three repeats performed for each condition.

Pattern	Number of cycles to spallation	Standard deviation
1	129	80
2	115	39
3	128	41
4	194	80
5	171	104
6	110	43
7	928	196
Ref.	882	253

According to EDX (energy dispersive X-ray) characterizations, it was possible to identify the darkest phase as alumina. Unfortunately, it is more difficult to define the other types of oxides, except that they could be $NiAl_2O_4$ spinel or even rutile $TiTaO_4$ according to the literature [23, 24]. If the layers of different oxides are systematically thicker than alumina, it is nevertheless impossible to correlate the thickness with oxide layers with the spallation life of the systems. Likewise, no correlation could be made between the lifetime and the nature of the oxides formed.

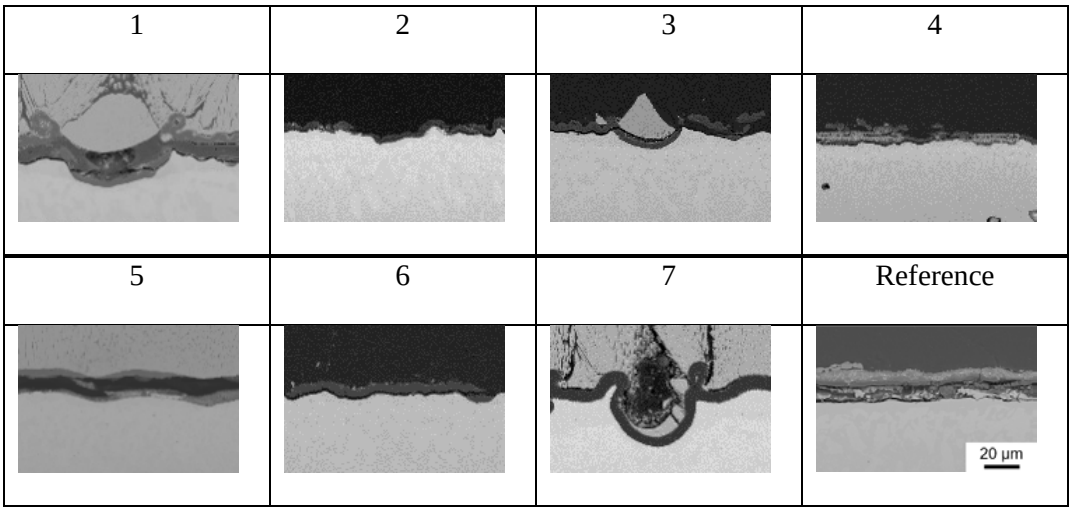

Figure 5: Oxides formed on the surfaces, cross-sectional views.

The evolution of the bond coat morphology is essential to understand the phenomena leading to the spallation of the ceramic layer. Firstly, it has been observed that the γ' precipitates within the bond coat tend to grow and coalesce (Fig. 6).

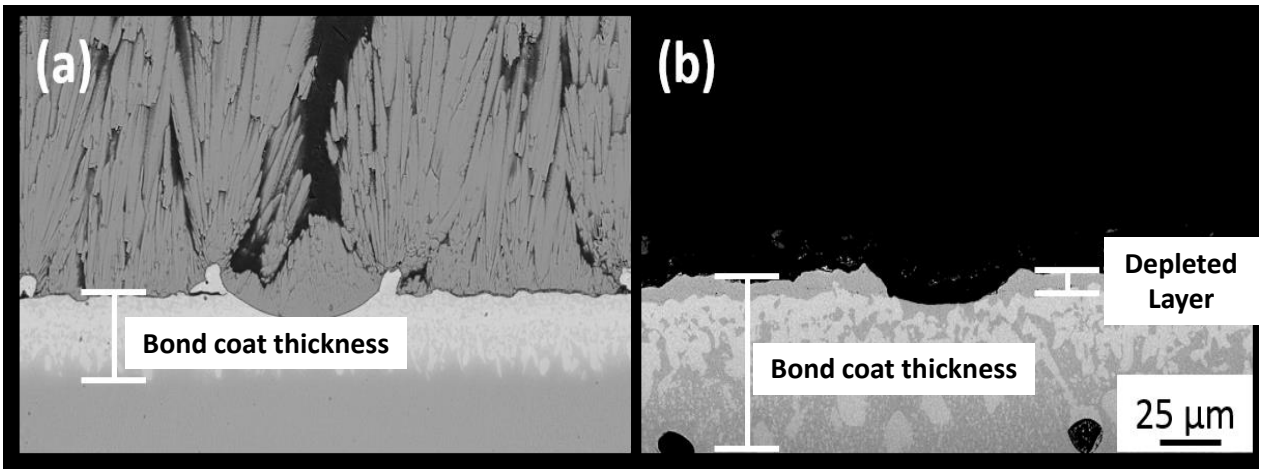

Figure 6: Thickness of the bond-coat (a) before and (b) after the oxidation cycling of 110 cycles at 1150°C.

In the same way, it appears that the diffusion front of the γ/γ' bond coat clearly evolves after the thermal cycling tests. Whatever the observed sample, a γ' depletion zone is systematically observed on the extreme surface of the layer (see Fig. 6(b)). By monitoring the thicknesses, it appears that the latter seem to be independent of the number of cycles and that the underlayers of morphology N°7 are those that have varied the most (x2.5). No rumpling phenomenon is to be noted here since this kind of bond coats are less prone to deformation by this type of phenomenon due, among other things, to their better resistance to creep in comparison to nickel-aluminide bond coats [20, 23]. In addition, the geometry of the material drops (growth) is also another marker, as the bond coat decreases during testing, deforming plastically. Here again, only morphology N°7 remains stable during the treatments and maintains its material beads despite the cycles undergone. Thus, with regard to the various notified evolutions, such as the growth of oxides of different natures, the size of these various oxide layers, the progress of the interdiffusion of the γ/γ' sub-layer towards

the superalloy, it is relevant to believe that the oxidation kinetics between the various studied thermal barrier systems differ. By thermogravimetric analyses, for 4 samples exposed for 100h at 1150°C, it is possible to notice that independently of the consideration of the surface morphology, the mass increases of samples 1, 7 and Ref are similar (Fig. 7). On the contrary, that of sample 5 (grid) is divided by a factor of 2, revealing the fact that the oxide layer develops less rapidly on this surface morphology. In this specific case, the entire surface was in fact affected by the laser texturing. These results therefore highlight the fact that laser treatment probably alters the chemistry at the extreme surface of the materials (and even more so in the so-called molten zones), which further modifies the growth kinetics and mechanisms of the oxides.

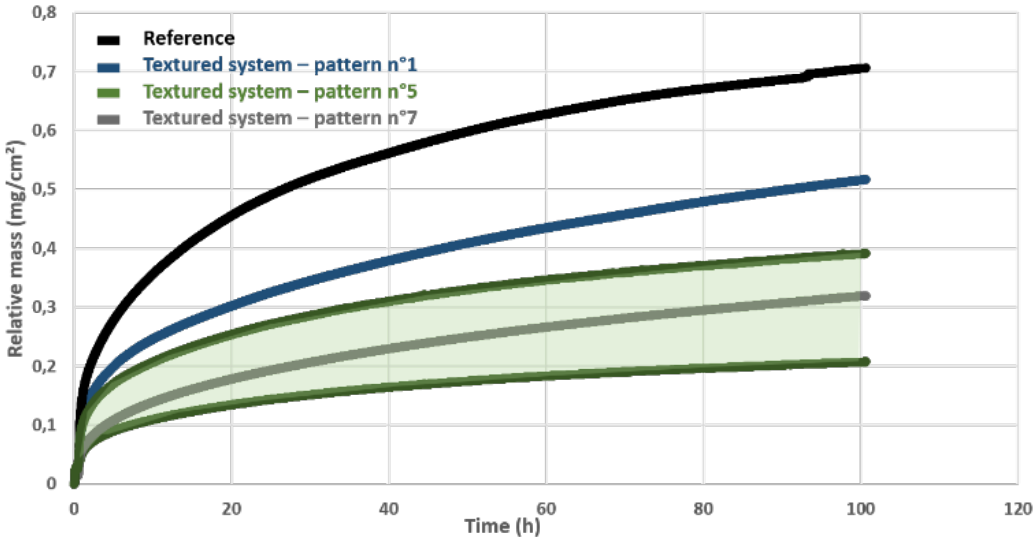

Figure 7: Evolution of the relative mass change of samples as a function of time at 1150°C for different surface morphologies- measurements of approximate surfaces (solid lines) or supposedly flat surfaces (dashed area).

According to these observations, it should appear from these results that a TBC system (sandblasted surfaces) oxidizes much faster than those on textured surfaces. This is particularly true for morphology N°7 where the time to spallation can be related to the relatively slow growth of the oxide layer. Compressive stresses within the TGO are thus minimized, thus slowing down spalling of the TC during cooling stages to relax the level on internal compressive stresses within the TGO [24, 25]. Concerning the grid morphology (pattern 5), the TC spalled very rapidly despite slow oxidation kinetics. It thus seems that the surface morphology is a main controlling factor of the thermal cycling life of this TBC system at 1150°C, in comparison to the apparent oxidation kinetics. Two main conclusions seem to stand out here, i.e., laser texturing modifies the oxidation kinetics of the thermal barrier systems and slowing down oxidation kinetics does not necessarily lead to a better thermal cycling life of the whole system.

Finally, test results have highlighted a surface morphology (Pattern 7) allowing to increase the spallation lifetime of multilayer systems. In order to confirm such results, out-of-phase thermal gradient mechanical fatigue (TGMF) tests were therefore carried out to get closer to the real solicitations.

According to Fig. 8, it is seen that specimens were macroscopically deforming in compression, in good agreement with the compressive stress applied during the hot part of the TGMF cycle. No plastic deformation seems to be accumulated during the tensile part of the cycle according to Fig. 8. Moreover, it can be seen that final failure occurred in a very brutal way at the end of the tests since no positive plastic deformation is observed for none of the curves in Fig. 8, indicating a very localized damage process. One has also to note that compared to previous similar tests done in similar conditions, but at Tmax = 1100 °C

using AM1 alloy [20], the present system using CMSX-4 Plus substrate presents a very limited compressive plastic strain.

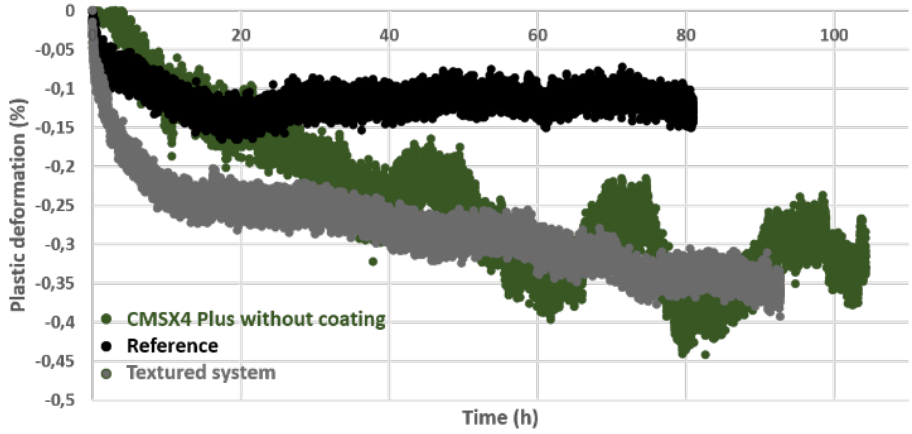

Figure 8: Plastic deformation of tubular specimens as a function of time.

Cracks leading to specimen failure always appear to start at the leading edge of the specimen, due to the locally highest temperature and are assisted by oxidation (Fig. 9). In fact, it seems that these cracks start in mode I, i.e., open cyclically during the tension phases of the TGMF cycle and oxidize during the hot stages of the cycles. Nevertheless, it would seem that cracks on the upstream side are developing at the thermal barrier coating/bond-coat interface, and do not propagate beyond the bond coat (not shown here). These fatigue cracks, perpendicular to the stress axis, have been observed by many authors when stressing TBC systems in thermomechanical fatigue [20, 26-29]. However, on the trailing edge, the cracks start from the ceramic layer and propagate within the sub-layer (Fig. 9).

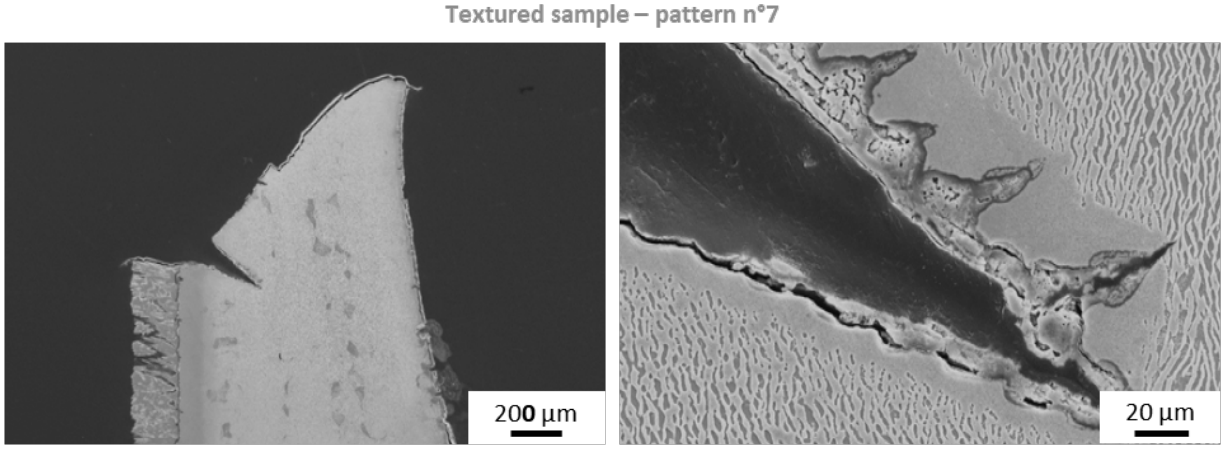

Figure 9: Cracks propagating from the outer surface of the specimen to the superalloy in the case of a CMSX4 plus/BC/TB system.

Some cracks in the specimen coated with a diffusion underlayer propagate even beyond the bond coat to the core of the superalloy, as already observed by Mauget et al, [20]. This tends to suggest a better resistance to crack propagation of the γ/γ' bond coat used in the present study. Thus, the texturing patterns are not preferential crack initiation zones despite their role as stress concentrators. Indeed, fatigue cracks initiating at the bond-coat/thermal barrier coating interface have also been observed to nucleate at the bottom of keyholes as well as in the areas not impacted by the laser treatment (Fig. 10).

From a more global point of view, laser texturing has been developed to slow down the spallation of the TC in order to increase the lifetime of coated specimens. It thus becomes relevant to evaluate the spallation resistance of the different systems when they are subjected to mechanical and thermal stresses close to that encountered in service. As shown in Fig. 11, the spallation mechanisms differ drastically between the thermal barrier system on sandblasted substrate and that on textured surface N°7. In fact, it turns out that all the gauge length of the upstream face of the specimen has spalled off on the leading edge for the reference sample whereas in the cases of textured samples, only the areas located in the edges of the samples, at the bottom of the specimens have spalled off (non-textured tubular areas during the texturing process).

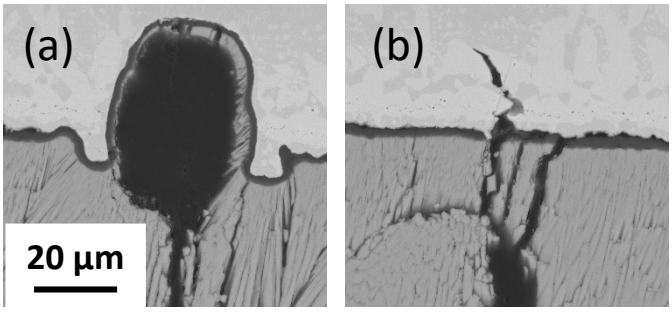

Figure 10: Surface cracks observed on: (a) leading edge of the "CMSX4 Plus / BC / TBC – N°7 pattern" specimen, (b) trailing edge of the "CMSX4 Plus / BC / TBC – N°7 pattern" specimen.

No mechanical anchoring is then provided in this part of the specimen, neither by texturing nor by sandblasting. The spalled parts of the textured specimens thus remain confined and no propagation of the spallation along the gage length could be observed.

In order to accelerate the spallation of the thermal barrier systems, by premature growth of the natural oxide layer, the coated specimens were then aged for 100 hours at 1150°C, in air, and the same results were noted. The entire gauge part of the reference specimen was impacted by this pre-aging that led to a full spallation at the bond coat/TGO interface of the TC (i.e., no more zirconia). Conversely, for textured parts, the spalled area remained limited to the edge of the sample, as already shown in Fig. 11, after this pre-aging. The crack leading to the spallation of the ceramic layer seems to have started within the TGO itself. The crack propagates through the oxide until it meets an obstacle, which are the material beads of the laser texturing patterns. The crack then continues to propagate slightly along the TGO/bond-coat interface until it is finally stopped by a material bead (Fig. 12). From the present experiments, it is understood that laser texturing has a main contribution in slowing down interfacial crack propagation between the TC and the BC, hence showing an interesting potential to improve the TBC system life in thermal cycling and/or TMF, providing that texturing parameters are optimized.

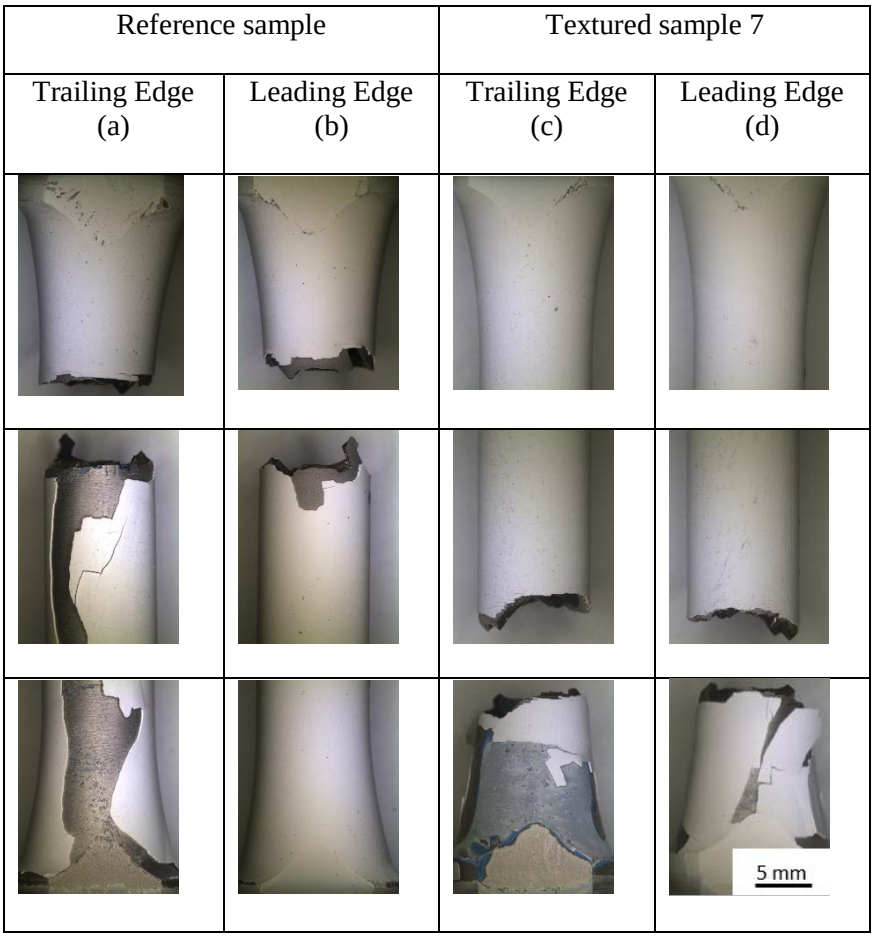

Figure 11: Scaling zones on unaged coated specimens: (a) reference, trailing edge; (b) reference, leading edge; (c) N°7 specimen, trailing edge; (d) specimen N°7, leading edge.

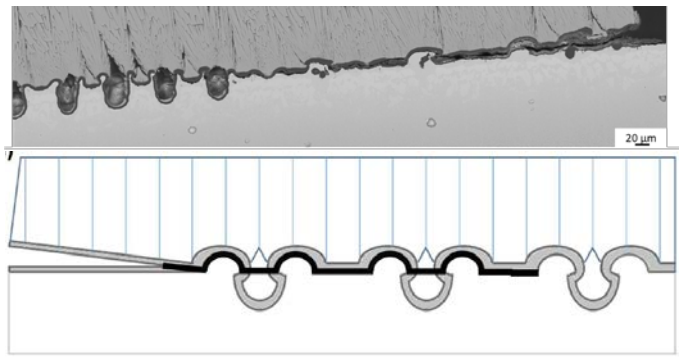

Figure 12: Observations and schematization of crack propagation on textured specimens seen in cross section.

4.0 CONCLUSIONS

The main objective of this work was to improve the durability of thermal barrier systems (CMSX4 Plus /γ/γ' BC/EB-PVD TBC) when they are subjected to complex thermomechanical stresses (i.e. cyclic oxidation

and thermal-gradient-mechanical fatigue). It was chosen, for this purpose, to reinforce the mechanical anchoring at the bond coat/topcoat interface by laser texturing. Indeed, this surface treatment process allows, by the principle of laser ablation, to model the extreme irradiated surface and thus control the interfacial roughness. Using this technology, it is possible to reach an infinite number of surface morphologies and different architectures have been tested in order to evaluate the spallation resistance of the systems. To do so, the spallation lifetime of the new textured systems was compared to a sandblasted system in thermal cycling test at 1150°C. Test results revealed only one promising surface morphology since all other configurations resulted in premature spallation of the ceramic layer in comparison with the reference system. During the TGMF tests in simulated engine environment, it seems that the morphologies developed by laser texturing reinforce the spallation resistance of thermal barrier systems. No propagation of the spallation could be observed along the gauge length of the textured tubular test tubes. Cracks leading to the spallation of the ceramic layer, which are initiated in the natural oxide layer and propagate along the TGO/BC interface, are stopped by the material beads of the textured patterns generated on the γ/γ' bond coat. Moreover, the texturing patterns do not appear to be preferred locations of crack initiation despite their stress concentrator character.

By further optimizing the texturing pattern of the bond coat, TBC life improvements in thermal cycling and in thermal-gradient-mechanical fatigue can be expected. Also, even if not mentioned here, the greater porosity induced in the ceramic top-coat by the bond-coat texturing provides a lower thermal conductivity and hence, better insulation during service, possibly allowing greater durability or harsher (hotter) temperature spikes like those encountered during post-combustion regimes. Still, a huge amount of work is required to adapt the laser texturing pattern to the exact thermo-mechanical fields of each components of the hot sections of aero-engines.

ACKNOWLEDGEMENTS

The authors gratefully acknowledge Safran Tech company for the financial support of this study. As well, CPER and FEDER (Region Nouvelle Aquitaine, Vienne Department, European Community, Poitiers Agglomeration and French Education and Research Ministry) financial supports are gratefully acknowledged.

REFERENCES

[1] O. Delcourt, “Material and Process Challenges for Aeronautical Equipment,” *Conference A3TS (french), 2016*.
[2] R.C. Reed, The Superalloys - Fundamentals and Applications, Cambridge University Press, (Cambridge UK, 2008).
[3] J. B. Wahl and K. Harris, “Improved 3rd Generation Single Crystal Superalloy CMSX-4®Plus (SLS)-a study of evolutionary alloy development,” Cannon-Muskegon Corp., (Muskegon Michigan, 1984).
[4] S. Tin and T. M. Pollock, “Phase Instabilities and Carbon Additions in Single-crystal Nickel-base Superalloys,” *Materials Science and Engineering A*, Vol. 348, No. 1–2, (2003), p. 111–121. doi:10.1016/S0921-5093(02)00637-8.
[5] J. Rame, S. Utada, L. Bortoluci Ormastroni, L. Mataveli Suave, E. Menou, L. Després, P.Kontis, and J. Cormier “Platinum Containing New Generation Nickel-based Superalloy for Single Crystalline Applications,” Superalloys, *TMS (2020)*, p 71–81. doi:10.1007/978-3-030-51834-9_7.
[6] S. Paquin and R. Cariou, “Turbine blade having an improved structure,” 2018 WO 2018/189434 A2 patent.
[7] A. Rollinger, R. Cariou, T. Flamme, S. Paquin, patent, “Turbine blade comprising a cooling circuit,” 2017 WO 2018/060627 A1

[8] D.R.Clarke, C.G.Levi, "Materials Design for The Next Generation ThermalBarrier Coatings", *Annual Review of Materials Research*, Vol. 33 (2003), p 383-471. doi: 10.1146/annurev.matsci.33.011403.113718

[9] M.H. Vidal-Setif, "Environmental Degradation of TBCs by Molten Deposits," *MRS Bulletin*, Vo. 37 (2012), p 932–941. doi:10.1557/mrs.2012.230

[10] J.L. Smialek, "Moisture-Induced Delayed Spallation and Interfacial Hydrogen Embrittlement of Alumina Scales," *J. of the Minerals, Metals and Materials Society*, Vol. 58, Issue 1, pp. 29-35. doi:10.1007/s11837-006-0064-2

[11] J.L. Smialek, "Improved Oxidation Life of Segmented Plasma Sprayed 8YSZ Thermal Barrier Coatings," *J. Thermal Spray Tech.*, Vol. 12, No. 1 (2004), p 66-75. doi: 10.1007/s11666-004-0051-5.

[9] J. Cormier, F. Mauget, J.B. Le Graverend, C. Moriconi, J. Mendez, "Issues related to the Constitutive Modeling of Ni-based Single Crystal Superalloys under Aeroengine Certification Conditions," *J. Aerospace Lab*, Issue 9 (2015), p. 1-13. doi :10.12762/2015.AL09-07.

[10] F. Mauget, D. Marchand, G. Benoit, M. Morisset, D. Bertheau, J. Cormier, J. Mendez, Z. Hervier, E. Ostoja-Kuczynski, C. Moriconi, "Development and Use of a New Burner Rig Facility to Mimic Service Loading Conditions of Ni-based Single Crystal Superalloys," *MATEC Web of Conferences, EUROSUPERALLOYS 2014 – 2nd European Symposium on Superalloys and their Applications*, Volume 14, (2014), p 2001. doi:10.1051/matecconf/20141420001

[11] F. Mauget, D. Marchand, M. Morisset, J. Mendez, "Nouveau moyen de caractérisation des matériaux Conditions extrêmes et sollicitations thermomécaniques proches des conditions d'usages," *Matériaux & Techniques*, Vol. 100, No. 6/7 (2012), p 541-545.

[12] R. Kromer, F. Mauget, L. Després, S. Costil, J. Cormier, "Thermo-mechanical Fatigue Evaluation of a Thermal Barrier Coating Bond-coatless System," *Materials Science and Engineering: A*, Vol. 756, (2019), p 130-141. doi:10.1016/j.msea.2019.04.020

[13] J. B. Wahl, K. Harris, "CMSX-4® Plus Single Crystal Alloy Development, Characterization and Application Development," *Superalloys 2016: Proceedings of the 13th International Symposium of Superalloys*, TMS (The Minerals, Metals & Materials Society), 2016, p 25-34. doi:10.1002/9781119075646.ch3

[14] H. E. Evans, "Oxidation Failure of TBC Systems: An Assessment of Mechanisms," *Surface and coatings Technology*, Vol. 206, Issue 7 (2011), p 1512–1521. doi:10.1016/j.surfcoat.2011.05.053

[15] G. Evans, D. R. Mumm, J. W. Hutchinson, G. H. Meier, and F. S. Pettit, "Mechanisms Controlling the Durability of Thermal Barrier Coatings," *Progress in Materials Science*, Vol. 46, (2001) p. 505–553. doi:10.1016/S0079-6425(00)00020-7

[16] V. K. Tolpygo and D. R. Clarke, "Surface Rumpling of a (Ni, Pt)Al Bond Coat Induced by Cyclic Oxidation," *Acta Materialia*, Vol. 48 (2000), p. 3283–3293. doi:10.1016/S1359-6454(00)00156-7

[20] F. Mauget, F. Hamon, M. Morisset, J. Cormier, F. Riallant, J. Mendez, "Damage Mechanisms in an EB-PVD Thermal Barrier Coating System during TMF and TGMF Testing Conditions under Combustion Environment," *Int. J. of Fatigue*, Vol. 99, Part 2 (2017), p 225-234. doi:10.1016/j.ijfatigue.2016.08.001

[21] C. S. Giggins, B. H. Kear, F. S. Pettit, and J. K. Tien, "Factors Affecting Adhesion of Oxide Scales on Alloys," *Metallurgical Transactions*, Vol. 5 (1974), p 1685–1688. doi:10.1007/BF02646343.

[17] E. P. Busso, Z. Q. Qian, M. P. Taylor, and H. E. Evans, "The Influence of Bond coat and Top coat Mechanical Properties on Stress Development in Thermal Barrier Coating Systems," *Acta Materialia*, Vol. 57 (2009), p. 2349–2361.- doi.org/10.1016/j.actamat.2009.01.017

[18] P. Audigie, PhD thesis, "Modélisation de l'interdiffusion et du comportement en oxydation cyclique de superalliages monocristallins à base nickel revetus d'une souscouche gamma-gamma' riche en platine. Extension aux systèmes barrières thermiques," Université de Toulouse, France, 2016.

[19] T. Izumi and B. Gleeson, "Oxidation Behavior of Pt + Hf-modified γ -Ni + γ'- Ni_3Al Alloys," *Materials Science Forum*, Vol. 522–523 (2006), p. 221–228. doi:10.4028/www.scientific.net/MSF.522-523.221

[20] A. Saboundji, V. Jaquet, L. M. Suave, and J. Rame, "Development of New Coating Compatible with Third-generation Nickel Based Superalloys and Thermal Barrier Coating," *Superalloys 2020*, TMS, 2020, p. 804–812.

[21] S. Selezneff, M. Boidot, J. Hugot, D. Oquab, C. Estournès, and D. Monceau, “Thermal Cycling Behavior of EBPVD TBC Systems deposited on Doped Pt-rich γ-γ’ Bond Coatings made by Spark Plasma Sintering (SPS),” *Surface and Coatings Technology*, Vol. 206, Issue 7 (2011), p 1558–1565. doi:10.1016/j.surfcoat.2011.06.011

[22] G. Evans, D. R. Mumm, J. W. Hutchinson, G. H. Meier, and F. S. Pettit, “Mechanisms Controlling the Durability of Thermal Barrier Coatings," *Progress in Materials Science*, Vol.46 (2001), p. 505–553. doi:10.1016/S0079-6425(00)00020-7

[23] A. Peichl, T. Beck, and O. Vöhringer, “Behaviour of an EB-PVD Thermal Barrier Coating System under Thermal-mechanical Fatigue Loading,” *Surface and Coatings Technology*, Vol. 162, Issues 2-3 (2003), p. 113–118. doi:10.1016/S0257-8972(02)00698-9

[24] Bickard, PhD thesis, “Endommagement sous sollicitations thermiques et mécaniques d'une barrière thermique et d'un aluminiure de nickel déposé sur un superalliage monocristallin,” Ecole Nationale Supérieure des Mines de Paris, France, 1998.